

Journal of Mechanics of Materials and Structures

**THERMAL BUCKLING AND FREE VIBRATION OF
TIMOSHENKO FG NANOBEMS BASED ON THE HIGHER-ORDER
NONLOCAL STRAIN GRADIENT THEORY**

Goran Janevski, Ivan Pavlović and Nikola Despenić

Volume 15, No. 1

January 2020



THERMAL BUCKLING AND FREE VIBRATION OF TIMOSHENKO FG NANOBELMS BASED ON THE HIGHER-ORDER NONLOCAL STRAIN GRADIENT THEORY

GORAN JANEVSKI, IVAN PAVLOVIĆ AND NIKOLA DESPENIĆ

A size-dependent Timoshenko beam model is derived within the framework of the higher-order nonlocal strain gradient theory. Nonlocal equations of motion are derived through Hamilton's principle and solved by applying an analytical solution. The solution is obtained using the Navier solution procedure. The paper investigates the thermal effects on buckling and free vibrational characteristics of functionally graded (FG) size-dependent nanobeams subjected to various types of thermal loading. The influence of higher-order and lower-order nonlocal parameters and strain gradient scale on buckling and vibration are investigated for various thermal conditions. To validate the solutions, the obtained results are compared with previous research.

1. Introduction

Thermal buckling of beams, as major solid structural components, has been the topic of many studies for a number of years. The development of functionally graded materials, which are a new type of materials, has attracted increasing attention recently. Structural elements such as beams in the micro or nanolength scale are commonly used as components in electromechanical systems. Therefore, understanding the mechanical properties of a functionally graded nanobeam in a thermal environment is necessary for its practical application.

There are various methods for static and dynamic analysis of nanostructures, such as molecular dynamics simulations [Neek-Amal and Peeters 2010; Alshehri and Hill 2017] and nonclassical continuum mechanics. Eringen's nonlocal elasticity theory [Eringen 1983; 2002] is one of the nonclassical continuum methods, which includes size-dependent effects, i.e., where stress at a reference point depends not only on the strain in this point but also on the strain in other points in the nearby region. The gradient elasticity theories [Aifantis 1992; Mindlin 1964] are also examples of the nonclassical continuum theories that can predict the stiffness enhancement effect. Based on the gradient elasticity theories, materials should be considered as atoms with a higher-order deformation mechanism at a small scale.

Lim et al. [2015] presented the higher-order nonlocal strain gradient theory starting from the point of view that the length scale present in the nonlocal elasticity and the strain gradient theory describe two entirely different physical characteristics. The nonlocal elasticity theory does not include nonlocality of higher-order stress. On the other hand, the strain gradient theory only considers local higher-order strain gradients. The higher-order nonlocal strain theory is primarily based on the nonlocal effects of the strain gradient field, i.e., nonlocal effects in a global sense.

Keywords: Timoshenko beam theory, thermal buckling, vibration, functionally graded materials, higher-order strain gradient theory.

Ebrahimi and Salari [2015a] studied the free vibration of an FG nanobeam subjected to an in-plane thermal loading. Material properties of the FG nanobeam vary along the thickness of the beam with power law gradation in the transversal direction. Using the Timoshenko beam theory, the authors considered the influence of the thermal effect, material distribution profile and small-scale effect based on the nonlocal elasticity theory of Eringen. The Navier type solution for a simply supported nanobeam was given for the first time. Temperature varied linearly as a function of thickness. For the same beam, as in the previous case, Ebrahimi and Salari [2016] studied the free vibration of the FG nanobeam where the temperature changed uniformly and varied linearly and nonlinearly.

The influence of the material distribution profile, thermal effect, small-scale effect, mode number and boundary conditions on the normalized natural frequencies of the temperature-dependent FG Euler–Bernoulli nanobeams was investigated in [Ebrahimi and Salari 2015b], where the nonlocal equations were solved by applying the differential transform method. Based on the nonlocal elasticity theory of Eringen, the authors considered the influence of the thermal effect, material distribution profile and small-scale effect, where the FG nanobeam was subjected to an in-plane thermal loading, which varied linearly and nonlinearly.

Li et al. [2016] studied the free vibration of an FG Timoshenko and Euler–Bernoulli nanobeam based on the nonlocal strain gradient theory. Material properties of the FG nanobeam depended on the through-thickness power-law variation of the two materials. The authors investigated the effect of the power-law and small length-scaled effect on natural frequencies of a simply supported FG nanobeam. In this paper, comparisons of the natural frequencies of Timoshenko and Euler beams were performed.

Xu et al. [2017] studied the bending and buckling of Euler–Bernoulli beams using the nonlocal strain gradient theory and the von Kármán nonlinear geometric relation.

Lu et al. [2017] studied the free vibration of the sinusoidal shear deformation of a nanobeam model based on the nonlocal strain gradient theory. Navier’s method was utilized to obtain analytical solutions for natural frequencies of simply supported nanobeams.

Trinh et al. [2016] presented an analytical method for vibration of a functionally graded beam under mechanical and thermal loads. The FG nanobeam was subjected to an in-plane thermal loading, where three types of temperature distribution through the thickness were taken into account: uniform temperature rise, linear temperature rise and nonlinear temperature rise. The effects of boundary conditions, temperature distributions and material parameters were investigated as well.

Chen et al. [2019] developed a nonlinear dynamical model for nonlocal strain gradient beams and analyzed its nonlinear free vibration. Based on the nonlocal strain gradient theory, the nonlinear governing equation of boundary conditions of the nanobeam was derived first. The effect of the slender ratio parameter, which might be also interpreted as the thickness-dependent size effect, was caused by the stress on account of the thickness-direction strain gradient. In the nonlinear free vibration analysis, an analytical solution for predicting the nonlinear free vibration frequencies was derived via the homotopy analysis method. It was shown that the nonlinear frequencies of the nanobeam display significant size-dependent phenomena for large values of the slender ratio parameter and either stiffness-softening or stiffness-hardening behavior might occur.

Based on the nonlocal strain gradient theory and various higher-order shear deformation theories, Alshujairi and Mollamahmutoğlu [2018] studied the buckling and free vibration of functionally graded sandwich microbeams resting on an elastic foundation. The authors reported on the effects of the nonlocal

parameter, the length scale parameter, gradient index, different cross-section shapes, temperature change and stiffnesses of Winkler and shear layer springs on the dimensionless critical buckling load and dimensionless frequencies.

In the manuscript [Ghazavi et al. 2018], the second strain gradient theory is applied to study the fluid-conveying Euler–Bernoulli nanotubes. Based on the high-order nonlocal strain gradient theory, Yang et al. [2018] studied the wave propagation behaviors of fluid-filled carbon nanotubes.

Ebrahimi and Haghi [2017] studied a rotating FG thermoelastic nanobeam under different temperature distributions. Based on the refined beam theory by using the nonlocal strain gradient theory, the authors analyzed the effects of temperature changes, angular velocity, nonlocal parameter, length scale parameter and material gradation on wave dispersion characteristics.

Pavlović et al. [2019a; 2019b] studied the stability and instability problem of a nanobeam subjected to the compressive axial load based on the higher-order nonlocal strain gradient theory. According to the direct Lyapunov method, the authors obtained the bounds of the almost sure asymptotic stability and instability, which was verified by numerical results using the Monte Carlo simulation method.

In this paper, size-dependent Timoshenko nanobeam models, which account for through-thickness power-law variation of two-constituent FG materials, will be deduced within the framework of the higher-order nonlocal strain gradient theory. This theory is employed to study effects of the buckling and vibrational behavior of nanobeams in different thermal environments. Equations of motion will be derived using Hamilton’s principle. By employing an analytical solution procedure, the closed-form critical buckling temperature and frequency will be obtained for simply supported boundary conditions. The obtained results are compared with the literature to confirm the validity of the solution. The influence of higher-order and lower-order nonlocal parameters and strain gradient scale on buckling and vibration will be investigated. Finally, certain important conclusions will be summarized.

2. Mathematical model

2.1. Problem description. Consider a nanobeam of functionally graded material, where the graded properties are assumed to be in the through-thickness direction. The system of interest is a rectangular functionally graded nanobeam of length L , width b and thickness h (Figure 1). The beam is subjected to an in-plane thermal loading, where, according to the rule of mixture, the effective material properties P_f are distributed as [Şimşek and Yurtcu 2013]

$$P_f(T, z) = P_c(T) V_c(z) + P_m(T) V_m(z), \quad (1)$$

where the volume fraction of the ceramic $V_c(z)$ and the volume fraction of the metal $V_m(z)$ constituent of the beam may be expressed using the power-law distribution

$$V_c(z) = \left(\frac{1}{2} + \frac{z}{h} \right)^P, \quad V_m(z) = 1 - V_c(z), \quad -\frac{h}{2} \leq z \leq \frac{h}{2}. \quad (2)$$

The temperature-dependent material properties (such as Young’s modulus E , thermal expansion coefficient α , mass density ρ , thermal conductivity κ and Poisson’s ratio ν) can be written as [Touloukian 1967]

$$P(T) = P_0(P_{-1}T^{-1} + 1 + P_1T + P_2T^2 + P_3T^3), \quad (3)$$

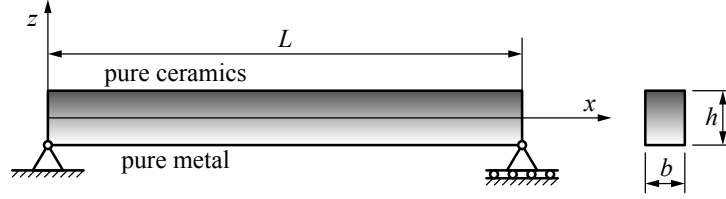


Figure 1. Geometry and coordinates of the functionally graded beam.

material	properties	P_0	P_{-1}	P_1	P_2	P_3
Si ₃ N ₄	E (Pa)	$348.4300 \cdot 10^9$	0	$-3.010 \cdot 10^{-4}$	$2.160 \cdot 10^{-7}$	$-8.946 \cdot 10^{-11}$
	α (K ⁻¹)	$5.8723 \cdot 10^{-6}$	0	$9.095 \cdot 10^{-4}$	0	0
	ρ (kg/m ³)	2370	0	0	0	0
	κ (W/mK)	13.723	0	$-1.032 \cdot 10^{-3}$	$5.466 \cdot 10^{-7}$	$-7.876 \cdot 10^{-11}$
	ν	0.24	0	0	0	0
SU 304	E (Pa)	$201.0400 \cdot 10^9$	0	$3.079 \cdot 10^{-4}$	$-6.534 \cdot 10^{-7}$	0
	α (K ⁻¹)	$12.3300 \cdot 10^{-6}$	0	$8.086 \cdot 10^{-4}$	0	0
	ρ (kg/m ³)	8166	0	0	0	0
	κ (W/mK)	15.3790	0	$-1.264 \cdot 10^{-3}$	$2.092 \cdot 10^{-6}$	$-7.223 \cdot 10^{-10}$
	ν	0.3262	0	$-2.002 \cdot 10^{-4}$	$3.797 \cdot 10^{-7}$	0

Table 1. Temperature-dependent coefficient of Young's modulus E , thermal expansion coefficient α , mass density ρ , thermal conductivity κ and Poisson's ratio ν for Si₃N₄ and SUS 304.

where P_0 , P_{-1} , P_1 , P_2 and P_3 are the coefficients that can be seen in the table of material properties for Si₃N₄ and SUS 304 (Table 1).

For the power-law distribution (2), the effective material properties are

$$P(z, T) = (P_c(T) - P_m(T)) \left(\frac{z}{h} + \frac{1}{2} \right)^P + P_m(T). \quad (4)$$

The bottom surface ($z = -h/2$) of the FG beam is pure metal (SUS 304) and the top surface ($z = h/2$) is pure ceramic (Si₃N₄).

2.2. The higher-order nonlocal strain gradient model for the FG nanobeam. Based on the higher-order nonlocal strain gradient theory [Lim et al. 2015], the nonlocal stress in a reference point x depends not only on the strain at that location but also on the strains in all other points in the nearby region. According to this theory, the internal strain energy density function can be expressed as

$$U_0 = \frac{1}{2} C_{ijkl} \varepsilon_{ij} \int_V \alpha_0(|x - x'|, e_0 a) \varepsilon'_{kl} dV' + \frac{l^2}{2} C_{ijkl} \varepsilon_{ij,m} \int_V \alpha_1(|x - x'|, e_1 a) \varepsilon'_{kl,m} dV', \quad (5)$$

where C_{ijkl} is the elastic modulus tensor of classical elasticity, ε_{ij} and ε'_{ij} are the Cartesian components of the strain tensor in points x and x' ; α_0 and α_1 are the kernel function related to the nonlocal effects

with respect to the strain field and the first order strain gradient field; e_0 and e_1 are the nonlocal material constants, a is the internal characteristic length and l is the strain gradient length scale parameter.

By using (5), the classical stress tensor $\boldsymbol{\sigma}$, the higher-order stress tensor $\boldsymbol{\sigma}^{(1)}$ and the total stress \boldsymbol{t} can be written as

$$\boldsymbol{\sigma} = \int_V \boldsymbol{\alpha}_0(|x-x'|, e_0 a) \boldsymbol{C} : \boldsymbol{\varepsilon}' dV', \quad \boldsymbol{\sigma}^{(1)} = l^2 \int_V \boldsymbol{\alpha}_1(|x-x'|, e_0 a) \boldsymbol{C} : \nabla \boldsymbol{\varepsilon}' dV', \quad \boldsymbol{t} = \boldsymbol{\sigma} - \nabla \boldsymbol{\sigma}^{(1)}. \quad (6)$$

In (6) the symbol “:” is used to denote the double-dot product. For an elastic material in the one-dimensional case, the generalized nonlocal constitutive relations in a differential form based on the higher-order nonlocal strain gradient theory may be simplified as

$$\left(1 - \mu_1 \frac{\partial^2}{\partial x^2}\right) \left(1 - \mu_0 \frac{\partial^2}{\partial x^2}\right) t_{xx} = E \left[\left(1 - \mu_1 \frac{\partial^2}{\partial x^2}\right) - l^2 \left(1 - \mu_0 \frac{\partial^2}{\partial x^2}\right) \frac{\partial^2}{\partial x^2} \right] \varepsilon_{xx}, \quad (7)$$

$$\left(1 - \mu_1 \frac{\partial^2}{\partial x^2}\right) \left(1 - \mu_0 \frac{\partial^2}{\partial x^2}\right) t_{xz} = G \left[\left(1 - \mu_1 \frac{\partial^2}{\partial x^2}\right) \frac{\partial^2}{\partial x^2} - l^2 \left(1 - \mu_0 \frac{\partial^2}{\partial x^2}\right) \frac{\partial^2}{\partial x^2} \right] \gamma_{xz}, \quad (8)$$

where $\mu_0 = (e_0 a)^2$ and $\mu_1 = (e_1 a)^2$. The normal and shear components of the total stress tensor of the nonlocal strain gradient theory are defined as

$$t_{xx} = \sigma_{xx} - \frac{\partial \sigma_{xx}^{(1)}}{\partial x}, \quad t_{xz} = \sigma_{xz} - \frac{\partial \sigma_{xz}^{(1)}}{\partial x}, \quad (9)$$

where σ_{xx} and σ_{xz} are the classical normal stress and classical shear stress components, $\sigma_{xx}^{(1)}$ and $\sigma_{xz}^{(1)}$ are the higher-order normal stress and higher-order shear stress components, ε_{xx} and γ_{xz} are the E normal strain and shear strain, E is Young's modulus, $G = E/2(1 + \nu)$ is the shear modulus, ν is Poisson's ratio. It is worth mentioning that for certain cases, the effect of structural thickness on the constitutive behaviors of nanostructures is studied in [Tang et al. 2019; Li et al. 2018; Chen et al. 2019].

2.3. Kinematic relations. The displacement components of any material point in the x , y and z direction can be written as

$$q_x = u(x, t) + z\varphi(x, t), \quad (10)$$

$$q_z = w(x, t), \quad (11)$$

where u and w are the displacement components of the mid-plane in the x and z direction, φ is the total bending rotation of the cross-section and t is the time. Using (10) and (11), the nonzero components of the beam are obtained as

$$\varepsilon_{xx} = \frac{\partial u}{\partial x} + z \frac{\partial \varphi}{\partial x}, \quad (12)$$

$$\gamma_{xz} = \frac{\partial w}{\partial x} + \varphi. \quad (13)$$

The governing equations of motion are obtained based on Hamilton's principle, which is expressed as

$$\int_{t_1}^{t_2} (\delta U + \delta V - \delta K) dt = 0, \quad (14)$$

in a time interval $t_1 < t < t_2$; δU is the virtual strain energy:

$$\begin{aligned} \delta U &= \int_V \left(\sigma_{xx} \delta \varepsilon_{xx} + \sigma_{xz} \delta \gamma_{xz} + \sigma_{xx}^{(1)} \frac{\partial(\delta \varepsilon_{xx})}{\partial x} + \sigma_{xz}^{(1)} \frac{\partial(\delta \varepsilon_{xz})}{\partial x} \right) dv \\ &= \int_L \left(N \delta \frac{\partial u}{\partial x} + M \delta \frac{\partial \varphi}{\partial x} + Q \delta \frac{\partial w}{\partial x} + Q \delta \varphi \right) dx + \left[N^{(1)} \delta \frac{\partial u}{\partial x} + M^{(1)} \delta \frac{\partial \varphi}{\partial x} + Q^{(1)} \delta \frac{\partial w}{\partial x} + Q^{(1)} \delta \varphi \right]_0^L. \end{aligned} \quad (15)$$

Here we consider the following stress resultant:

$$\begin{aligned} N &= \int_A t_{xx} dA, & M &= \int_A z t_{xx} dA, & Q &= k_s \int_A t_{xz} dA, \\ N^{(1)} &= \int_A \sigma_{xx}^{(1)} dA, & M^{(1)} &= \int_A z \sigma_{xx}^{(1)} dA, & Q^{(1)} &= k_s \int_A \sigma_{xz}^{(1)} dA, \end{aligned} \quad (16)$$

where $k_s = \frac{5}{6}$ is the shear correction factor; δV is the variation of the work by thermal expansion:

$$\delta V = - \int_V E(T, z) \alpha(T, z) (T - T_0) \frac{\partial w}{\partial x} \frac{\partial}{\partial x} (\delta w) dv = - \int_0^L \left(N^T \frac{\partial w}{\partial x} \frac{\partial}{\partial x} (\delta w) \right) dx, \quad (17)$$

where N^T is the thermal resultant:

$$N^T = \int_{-h/2}^{h/2} E(T, z) \alpha(T, z) (T - T_0) b dz, \quad (18)$$

and $T_0 = 300$ K is the reference temperature; δK is the virtual kinetic energy:

$$\begin{aligned} \delta K &= \frac{1}{2} \int_V \rho(T, z) \delta \left[\left(\frac{\partial q_x}{\partial t} \right)^2 + \left(\frac{\partial q_z}{\partial t} \right)^2 \right] dv \\ &= \int_0^L \left\{ I_0 \left[\frac{\partial u}{\partial t} \delta \left(\frac{\partial u}{\partial t} \right) + \frac{\partial w}{\partial t} \delta \left(\frac{\partial w}{\partial t} \right) \right] + I_1 \left[\frac{\partial \varphi}{\partial t} \delta \left(\frac{\partial u}{\partial t} \right) + \frac{\partial u}{\partial t} \delta \left(\frac{\partial \varphi}{\partial t} \right) \right] + I_2 \frac{\partial \varphi}{\partial t} \delta \left(\frac{\partial \varphi}{\partial t} \right) \right\} dx, \end{aligned} \quad (19)$$

where the mass moments of inertia are defined as

$$(I_0, I_1, I_2) = \int_A (1, z, z^2) \rho(z, T) dA. \quad (20)$$

By substituting (15), (17) and (19) into (14), using integration by parts and setting the coefficients of δu , δw , $\delta \varphi$ to zero, one obtains the following governing equations of motion based on the Timoshenko beam theory

$$\delta u: \frac{\partial N}{\partial x} = I_0 \frac{\partial^2 u}{\partial t^2} + I_1 \frac{\partial^2 \varphi}{\partial t^2}, \quad (21)$$

$$\delta w: \frac{\partial Q}{\partial x} - N^T \frac{\partial^2 w}{\partial x^2} = I_0 \frac{\partial^2 w}{\partial t^2}, \quad (22)$$

$$\delta \varphi: \frac{\partial M}{\partial x} - Q = I_1 \frac{\partial^2 u}{\partial t^2} + I_2 \frac{\partial^2 \varphi}{\partial t^2}, \quad (23)$$

with the classical boundary conditions (at $x = 0$ or $x = L$)

$$\delta u: N = 0, \quad \text{or } u = 0, \quad (24)$$

$$\delta w: Q - N^T \frac{\partial w}{\partial x} = 0, \quad \text{or } w = 0, \quad (25)$$

$$\delta \varphi: M = 0, \quad \text{or } \varphi = 0, \quad (26)$$

and the nonclassical boundary conditions (at $x = 0$ or $x = L$)

$$\delta \frac{\partial u}{\partial x}: N^{(1)} = 0, \quad \text{or } \frac{\partial u}{\partial x} = 0, \quad (27)$$

$$\delta \left(\frac{\partial w}{\partial x} + \varphi \right): Q^{(1)} = 0, \quad \text{or } \frac{\partial w}{\partial x} + \varphi = 0, \quad (28)$$

$$\delta \frac{\partial \varphi}{\partial x}: M^{(1)} = 0, \quad \text{or } \frac{\partial \varphi}{\partial x} = 0. \quad (29)$$

Considering the above and integrating (7) and (8) over the beam's cross-section, the force-strain and moment-strain relation can be obtained as

$$\begin{aligned} \left(1 - \mu_1 \frac{\partial^2}{\partial x^2}\right) \left(1 - \mu_0 \frac{\partial^2}{\partial x^2}\right) N = A_{xx} \left[\left(1 - \mu_1 \frac{\partial^2}{\partial x^2}\right) - l^2 \left(1 - \mu_0 \frac{\partial^2}{\partial x^2}\right) \frac{\partial^2}{\partial x^2} \right] \frac{\partial u}{\partial x} \\ + B_{xx} \left[\left(1 - \mu_1 \frac{\partial^2}{\partial x^2}\right) - l^2 \left(1 - \mu_0 \frac{\partial^2}{\partial x^2}\right) \frac{\partial^2}{\partial x^2} \right] \frac{\partial \varphi}{\partial x}, \end{aligned} \quad (30)$$

$$\begin{aligned} \left(1 - \mu_1 \frac{\partial^2}{\partial x^2}\right) \left(1 - \mu_0 \frac{\partial^2}{\partial x^2}\right) M = B_{xx} \left[\left(1 - \mu_1 \frac{\partial^2}{\partial x^2}\right) - l^2 \left(1 - \mu_0 \frac{\partial^2}{\partial x^2}\right) \frac{\partial^2}{\partial x^2} \right] \frac{\partial u}{\partial x} \\ + D_{xx} \left[\left(1 - \mu_1 \frac{\partial^2}{\partial x^2}\right) - l^2 \left(1 - \mu_0 \frac{\partial^2}{\partial x^2}\right) \frac{\partial^2}{\partial x^2} \right] \frac{\partial \varphi}{\partial x}, \end{aligned} \quad (31)$$

$$\left(1 - \mu_1 \frac{\partial^2}{\partial x^2}\right) \left(1 - \mu_0 \frac{\partial^2}{\partial x^2}\right) Q = C_{xz} \left[\left(1 - \mu_1 \frac{\partial^2}{\partial x^2}\right) - l^2 \left(1 - \mu_0 \frac{\partial^2}{\partial x^2}\right) \frac{\partial^2}{\partial x^2} \right] \left(\frac{\partial w}{\partial x} + \varphi \right), \quad (32)$$

in which the cross-sectional rigidities are

$$(A_{xx}, B_{xx}, D_{xx}) = \int_A (1, z, z^2) E(z, T) dA, \quad C_{xz} = k_s \int_A G(z, T) dA. \quad (33)$$

We introduce the following dimensionless parameters

$$\xi = \frac{x}{L}, \quad U(\xi, \tau) = \frac{u(x, t)}{L}, \quad W(\xi, \tau) = \frac{w(x, t)}{L}, \quad \tau = \frac{t}{L^2} \sqrt{\frac{E_c(T_c) I}{\rho_c(T_c) A}}, \quad (34)$$

where $E_c(T_c)$ and $\rho_c(T_c)$ are Young's modulus and the mass density of ceramic Si_3N_4 at the temperature T_c , $I = \frac{1}{12}bh^3$ is the moment of inertia of the rectangular cross-section of the beam and $A = bh$. The explicit relation of the nonlocal normal force, bending moment and shear force can be derived by

substituting the second and fourth derivative of these values from (21)÷(23) into (30)÷(32) as

$$N = A_{xx} \left\{ \mathcal{L}_{(3)} \left[\frac{\partial U}{\partial \xi} + k_B \frac{\partial \varphi}{\partial \xi} \right] + k_I \mathcal{L}_{(2)} \left[k_{I0} \frac{\partial^3 U}{\partial \xi \partial \tau^2} + k_{I1} \frac{\partial^3 \varphi}{\partial \xi \partial \tau^2} \right] \right\}, \quad (35)$$

$$M = A_{xx} L \left\{ \mathcal{L}_{(3)} \left[k_B \frac{\partial U}{\partial \xi} + k_D \frac{\partial \varphi}{\partial \xi} \right] + \mathcal{L}_{(2)} \left[k_N \frac{\partial^2 W}{\partial \xi^2} + k_I k_{I0} \frac{\partial^2 W}{\partial \tau^2} + k_I k_{I1} \frac{\partial^3 U}{\partial \xi \partial \tau^2} + k_I k_{I2} \frac{\partial^3 \varphi}{\partial \xi \partial \tau^2} \right] \right\}, \quad (36)$$

$$Q = A_{xx} \left\{ k_C \mathcal{L}_{(3)} \left[\frac{\partial W}{\partial \xi} + \varphi \right] + \mathcal{L}_{(2)} \left[k_I k_{I0} \frac{\partial^3 W}{\partial \xi \partial \tau^2} + k_N \frac{\partial^3 W}{\partial \xi^3} \right] \right\}, \quad (37)$$

where the linear differential operators are

$$\begin{aligned} \mathcal{L}_{(0)} &= 1 - k_{\mu 0} \nabla^2, & \mathcal{L}_{(1)} &= 1 - k_{\mu 1} \nabla^2, & \mathcal{L}_{(2)} &= (k_{\mu 0} + k_{\mu 1}) - k_{\mu 0} k_{\mu 1} \nabla^2, \\ \mathcal{L}_{(3)} &= \mathcal{L}_{(1)} - k_I \mathcal{L}_{(0)} \nabla^2 = 1 - (k_{\mu 1} + k_I) \nabla^2 + k_{\mu 0} k_I \nabla^4, & \nabla &= \frac{\partial}{\partial \xi}, \end{aligned} \quad (38)$$

and the marks are

$$\begin{aligned} k_B &= \frac{B_{xx}}{A_{xx} L}, & k_C &= \frac{C_{xz}}{A_{xx}}, & k_D &= \frac{D_{xx}}{A_{xx} L^2}, & k_N &= \frac{N^T}{A_{xx}}, \\ k_I &= \frac{I}{AL^2}, & k_{I0} &= \frac{E_c(T_c) I_0}{\rho_c(T_c) A_{xx}}, & k_{I1} &= \frac{E_c(T_c) I_1}{\rho_c(T_c) A_{xx} L}, & k_{I2} &= \frac{E_c(T_c) I_2}{\rho_c(T_c) A_{xx} L^2}, \\ & & k_I &= \frac{l^2}{L^2}, & k_{\mu 0} &= \frac{\mu_0}{L^2}, & k_{\mu 1} &= \frac{\mu_1}{L^2}. \end{aligned} \quad (39)$$

Substituting the derivative for N , M and Q from (35)÷(37) into (21)÷(23), the nonlocal governing equations of the Timoshenko FG nanobeam can be derived as

$$\mathcal{L}_{(3)} \left[\frac{\partial^2 U}{\partial \xi^2} + k_B \frac{\partial^2 \varphi}{\partial \xi^2} \right] - k_I \mathcal{L}_{(4)} \left[k_{I0} \frac{\partial^2 U}{\partial \tau^2} + k_{I1} \frac{\partial^2 \varphi}{\partial \tau^2} \right] = 0, \quad (40)$$

$$\mathcal{L}_{(3)} \left[k_B \frac{\partial^2 U}{\partial \xi^2} + k_D \frac{\partial^2 \varphi}{\partial \xi^2} - k_C \left(\frac{\partial W}{\partial \xi} + \varphi \right) \right] - k_I \mathcal{L}_{(4)} \left[k_{I1} \frac{\partial^2 U}{\partial \tau^2} + k_{I2} \frac{\partial^2 \varphi}{\partial \tau^2} \right] = 0, \quad (41)$$

$$k_C \mathcal{L}_{(3)} \left[\frac{\partial^2 W}{\partial \xi^2} + \frac{\partial \varphi}{\partial \xi} \right] - k_N \mathcal{L}_{(4)} \left[\frac{\partial^2 W}{\partial \xi^2} \right] - k_I k_{I0} \mathcal{L}_{(4)} \left[\frac{\partial^2 W}{\partial \tau^2} \right] = 0, \quad (42)$$

where the linear differential operator is $\mathcal{L}_{(4)} = \mathcal{L}_{(0)} \mathcal{L}_{(1)} = 1 - (k_{\mu 0} + k_{\mu 1}) \nabla^2 + k_{\mu 0} k_{\mu 1} \nabla^4$.

2.4. Temperature rise. In the case of a uniform temperature rise (UTR), the temperature of the FG beam uniformly rises by ΔT . Since the temperature is constant in the z -direction, then

$$T(z) = T_0 + \Delta T = \text{const}. \quad (43)$$

In the case of a linear temperature rise (LTR), the temperature of the FG beam varies linearly along the thickness of the beam

$$T(z) = T_m + \Delta T \left(\frac{1}{2} + \frac{z}{h} \right), \quad (44)$$

where the temperature of the top and the bottom surface of the nanobeam are

$$T_c = T(h/2), \quad T_m = T(-h/2), \quad (45)$$

where $\Delta T = T_c - T_m$. In this paper, it is assumed that the temperature of the bottom surface is $T_m = T_0 + 5 = 305$ K.

In the case of heat conduction across the thickness, the temperature of the FG nanobeam varies non-linearly (NLTR) along the thickness of the beam. The one-dimensional steady state heat conduction problem can be formulated by a differential equation [Fu et al. 2012]

$$\frac{d}{dz} \left(\kappa(z, T) \frac{dT(z)}{dz} \right) = 0, \quad (46)$$

where the known temperature boundary conditions on the bottom and the top surface are given as in (45). In order to present an analytical solution for (46), it is common to assume that thermal conductivity $\kappa = \kappa(z)$ is independent of temperature. Taking this into account, the solution of (46) can be obtained in a power series as

$$T(z) = T_m + \frac{\Delta T}{\lambda} \sum_{i=0}^n \frac{1}{ki+1} \left(\frac{1}{2} + \frac{z}{h} \right)^{ki+1} \left(\frac{\kappa_m - \kappa_c}{\kappa_m} \right)^i, \quad (47)$$

where

$$\lambda = \sum_{i=0}^n \frac{1}{ki+1} \left(\frac{\kappa_m - \kappa_c}{\kappa_m} \right)^i. \quad (48)$$

2.5. Solution procedures. This section presents the analytical solutions for the vibration problem described by equations (40)–(42). The Navier solution approach will be used to determine the analytical solutions of vibration frequencies and critical buckling temperature for simply supported boundary conditions. In the case of simply supported boundary conditions, one should specify the classical boundary conditions

$$N = 0, \quad w = 0, \quad \text{and} \quad M = 0, \quad (\text{at } \xi = 0 \text{ and } \xi = 1). \quad (49)$$

As stated above, we consider the nonclassical boundary conditions in the case of the Timoshenko beam

$$\frac{\partial u}{\partial x} = 0, \quad Q^{(1)} = 0, \quad \text{and} \quad \frac{\partial \varphi}{\partial x} = 0, \quad (\text{at } \xi = 0 \text{ and } \xi = 1). \quad (50)$$

By using (6), (9) and (12), $Q^{(1)}$ can be obtained in the displacement form

$$Q^{(1)} = A_{xx} \left\{ k_C \left[\frac{k_{\mu 1}^2}{k_{\mu 0} - k_{\mu 1}} \mathcal{L}_{(0)} \mathcal{L}_{(3)} - \frac{k_{\mu 1}^2 - k_l^2 (k_{\mu 0} - k_{\mu 1})}{k_{\mu 0} - k_{\mu 1}} \left(1 - \frac{k_{\mu 0} k_{\mu 1} k_l^2}{k_{\mu 1}^2 - k_l^2 (k_{\mu 0} - k_{\mu 1})} \nabla^2 \right) \right] \left(\frac{\partial^2 W}{\partial \xi^2} + \frac{\partial \varphi}{\partial \xi} \right) + \frac{k_{\mu 1}^2}{k_{\mu 0} - k_{\mu 1}} \mathcal{L}_{(1)} \mathcal{L}_{(2)} \left(k_I k_{I0} \frac{\partial^3 W}{\partial \xi \partial \tau^2} + k_N \frac{\partial^3 W}{\partial \xi^3} \right) \right\}. \quad (51)$$

The displacement functions can be assumed to be periodic in time in the form

$$U(\xi, \tau) = \sum_{n=1}^{\infty} U_n \cos(n\pi\xi) e^{i\omega_n\tau}, \quad (52)$$

$$W(\xi, \tau) = \sum_{n=1}^{\infty} W_n \sin(n\pi\xi) e^{i\omega_n\tau}, \quad (53)$$

$$\varphi(\xi, \tau) = \sum_{n=1}^{\infty} \varphi_n \cos(n\pi\xi) e^{i\omega_n\tau}, \quad (54)$$

where $i = \sqrt{-1}$, U_j, W_j, φ_j ($j = 1, 2, \dots, n$) are the unknown Fourier coefficients to be determined for each n value and ω_n is the frequency of vibration. It can be checked that the series solution (52)÷(54) satisfies the classical boundary conditions (24)÷(26) and nonclassical boundary conditions (27)÷(29).

Eliminating U and φ from (40)÷(42), the governing differential equation becomes

$$\mathcal{L}_{(8)}(\mathcal{L}_{(5)}\mathcal{L}_{(7)} - \mathcal{L}_{(6)}^2)W + k_C^2 \mathcal{L}_{(3)}^2 \mathcal{L}_{(5)} \frac{\partial^2 W}{\partial \xi^2} = 0, \quad (55)$$

where the linear differential operators are

$$\mathcal{L}_{(5)} = \mathcal{L}_{(3)}\nabla^2 - k_I k_{I0} \mathcal{L}_{(4)} \frac{\partial^2}{\partial \tau^2}, \quad \mathcal{L}_{(6)} = k_B \mathcal{L}_{(3)}\nabla^2 - k_I k_{I1} \mathcal{L}_{(4)} \frac{\partial^2}{\partial \tau^2}, \quad (56)$$

$$\mathcal{L}_{(7)} = k_D \mathcal{L}_{(3)}\nabla^2 - k_C \mathcal{L}_{(3)} - k_I k_{I2} \mathcal{L}_{(4)} \frac{\partial^2}{\partial \tau^2}, \quad \mathcal{L}_{(8)} = (k_C \mathcal{L}_{(3)} - k_N \mathcal{L}_{(4)})\nabla^2 - k_I k_{I0} \mathcal{L}_{(4)} \frac{\partial^2}{\partial \tau^2}. \quad (57)$$

Substituting (53) into (55) and neglecting the coefficient of ω_n^6 , we get the following characteristic equation

$$\alpha_4^2 A_\omega \omega_n^4 + \alpha_3 \alpha_4 B_\omega \omega_n^2 + \alpha_3^2 C_\omega = 0, \quad (58)$$

where

$$\begin{aligned} A_\omega &= -k_I^2 [(\alpha_1 \alpha_6 + \alpha_3 \alpha_5 k_{I0}) n^2 \pi^2 + \alpha_3 k_C k_{I0}^2], \\ B_\omega &= k_I [(\alpha_2 \alpha_3 k_{I0} + \alpha_1 \alpha_5) n^4 \pi^4 - k_C k_{I0} (\alpha_3 - k_N \alpha_4)] n^2 \pi^2, \\ C_\omega &= k_C k_N \alpha_4 n^4 \pi^4 - \alpha_1 \alpha_2 n^6 \pi^6, \\ \alpha_1 &= k_C \alpha_3 - k_N \alpha_4, \\ \alpha_2 &= k_D - k_B^2, \\ \alpha_3 &= 1 + (k_{\mu 1} + k_I) n^2 \pi^2 + k_{\mu 0} k_I n^4 \pi^4, \\ \alpha_4 &= 1 + (k_{\mu 0} + k_{\mu 1}) n^2 \pi^2 + k_{\mu 0} k_{\mu 1} n^4 \pi^4, \\ \alpha_5 &= k_{I2} - 2k_B k_{I1} + k_D k_{I0}, \\ \alpha_6 &= k_{I0} k_{I2} - k_{I1}^2. \end{aligned} \quad (59)$$

The smaller root (the eigenvalue $\lambda_n = \omega_n^2$) of (58) is

$$\omega_n^2 = \frac{\alpha_3}{\alpha_4} \frac{-B_\omega + \sqrt{B_\omega^2 - 4A_\omega C_\omega}}{2A_\omega}. \quad (60)$$

By setting the fundamental frequency ω_1 to zero, we find the critical buckling temperature ΔT_{cr} (for $n = 1$). This condition is satisfied if the coefficient $C_\omega = 0$. After a simple transformation, we come to a relation among the parameters of the system that meets the required condition

$$k_I = \frac{1 + k_{\mu 1} n^2 \pi^2}{1 + k_{\mu 0} n^2 \pi^2} \frac{k_N (1 + k_{\mu 0} n^2 \pi^2) (k_C + \alpha_2 n^2 \pi^2) - k_C \alpha_2 n^2 \pi^2}{k_C \alpha_2 n^4 \pi^4}. \quad (61)$$

It is interesting that the parameters of the system (59) can be simplified to certain interesting cases:

Case 1 (Eringen's nonlocal continuum theory). In the case where the strain gradient length scale ($l = 0$) and the nonlocal parameter ($\mu_1 = 0$) are zero, the parameters of system (59) are

$$\begin{aligned} A_\omega &= -k_I^2 \{k_C k_{I0}^2 + n^2 \pi^2 [k_{I0} \alpha_5 + k_C \alpha_6 - k_N \alpha_6 (1 + k_{\mu 0} n^2 \pi^2)]\}, \\ B_\omega &= k_I n^2 \pi^2 [k_C k_{I0} + n^2 \pi^2 (k_{I0} \alpha_2 + k_C \alpha_5) - k_N (1 + k_{\mu 0} n^2 \pi^2) (k_C k_{I0} + \alpha_5 n^2 \pi^2)], \\ C_\omega &= n^4 \pi^4 [k_N (1 + k_{\mu 0} n^2 \pi^2) (k_C + \alpha_2 n^2 \pi^2) - k_C \alpha_2 n^2 \pi^2], \\ \frac{\alpha_3}{\alpha_4} &= \frac{1}{1 + k_{\mu 0} n^2 \pi^2}. \end{aligned} \quad (62)$$

By setting the strain gradient length scale ($l = 0$) and the nonlocal parameter ($\mu_1 = 0$) to zero we can find the critical temperature ΔT_{cr} from (61) as

$$k_{\mu 0} = \frac{\alpha_2 n^2 \pi^2 (k_C - k_N) - k_C k_N}{k_N n^2 \pi^2 (k_C + \alpha_2 n^2 \pi^2)}. \quad (63)$$

Case 2 (classical continuum theory). In the case where the strain gradient length scale ($l = 0$) and the nonlocal parameters ($\mu_0 = 0$, $\mu_1 = 0$) are zero, the parameters of the system are

$$\begin{aligned} A_\omega &= -k_I^2 \{k_C k_{I0}^2 + n^2 \pi^2 [k_{I0} \alpha_5 + \alpha_6 (k_C - k_N)]\}, \\ B_\omega &= k_I n^2 \pi^2 \{k_C k_{I0} (1 - k_N) + n^2 \pi^2 [k_{I0} \alpha_2 + \alpha_5 (k_C - k_N)]\}, \\ C_\omega &= n^4 \pi^4 [k_C k_N - \alpha_2 n^2 \pi^2 (k_C - k_N)], \\ \frac{\alpha_3}{\alpha_4} &= 1. \end{aligned} \quad (64)$$

In a special case of the homogenous beam, based on expressions (20), (33) and (39), one can obtain

$$k_{I0} = 1, \quad k_{I1} = 0, \quad k_{I2} = k_I, \quad k_B = 0, \quad k_C = \frac{k_s}{2(1 + \nu)}, \quad k_D = k_I. \quad (65)$$

Based on expressions (60), (64) and (65), the frequencies of the beam can be derived as

$$\omega_n^2 = \frac{1}{2k_I^2} \frac{k_s k_I n^2 \pi^2 (1 - k_N) + 2k_I^2 n^4 \pi^4 [1 + \nu + k_s - 2k_N (1 + \nu)] - k_I n^2 \pi^2 \sqrt{D}}{k_s + k_I n^2 \pi^2 [k_s + 2(1 + \nu)(2 - k_N)]}, \quad (66)$$

where

$$D = [k_s(1+k_N) + 2k_I n^2 \pi^2 (1+\nu)]^2 + 8k_N k_I n^2 \pi^2 (1+\nu) [k_s + 2k_I n^2 \pi^2 (1+\nu)] - 8k_s k_I^2 n^4 \pi^4 (1+\nu). \quad (67)$$

Finally, in the case when the homogenous beam is without a thermal environment ($k_N = 0$), the frequencies of the beam can be derived as

$$\omega_n^2 = \frac{1}{2k_I^2} \frac{k_s k_I n^2 \pi^2 + 2k_I^2 n^4 \pi^4 (1+\nu+k_s) - k_I n^2 \pi^2 \sqrt{[k_s + 2k_I n^2 \pi^2 (1+\nu)]^2 - 8k_s k_I^2 n^4 \pi^4 (1+\nu)}}{k_s + k_I n^2 \pi^2 [k_s + 4(1+\nu)]}. \quad (68)$$

Case 3. In the case where the strain gradient length scale ($l = 0$) is zero, the parameters of the system are

$$\begin{aligned} A_\omega &= -k_I^2 (1 + k_{\mu_1} n^2 \pi^2) \{k_C k_{I0}^2 - n^2 \pi^2 [k_N \alpha_6 (1 + k_{\mu_0} n^2 \pi^2) - k_C \alpha_6 - k_{I0} \alpha_5]\}, \\ B_\omega &= k_I n^2 \pi^2 (1 + k_{\mu_1} n^2 \pi^2) [k_C k_{I0} + k_{I0} \alpha_2 n^2 \pi^2 + k_C \alpha_5 n^2 \pi^2 - k_N (1 + k_{\mu_0} n^2 \pi^2) (k_C k_{I0} + \alpha_5 n^2 \pi^2)], \\ C_\omega &= n^4 \pi^4 (1 + k_{\mu_1} n^2 \pi^2) [k_N (1 + k_{\mu_0} n^2 \pi^2) (k_C + \alpha_2 n^2 \pi^2) - k_C \alpha_2 n^2 \pi^2], \\ \frac{\alpha_3}{\alpha_4} &= \frac{1}{1 + k_{\mu_0} n^2 \pi^2}. \end{aligned} \quad (69)$$

It is noticeable that in this case the natural frequency does not depend on the nonlocal parameters μ_1 , but only on the parameter μ_0 . By setting the strain gradient length scale ($l = 0$) to zero we can find the critical temperature ΔT_{cr} from (61) as

$$k_{\mu_0} = \frac{\alpha_2 n^2 \pi^2 (k_C - k_N) - k_C k_N}{k_N n^2 \pi^2 (k_C + \alpha_2 n^2 \pi^2)}. \quad (70)$$

It is noticeable that in this case the critical temperature ΔT_{cr} does not depend on the nonlocal parameters μ_1 , but only on the parameter μ_0 , and is the same as the one we can determine from conditions (63) in Case 1.

Case 4 (lower-order nonlocal strain gradient theory). In the case where the nonlocal parameters are equal ($\mu_1 = \mu_0$) the parameters of the system are

$$\begin{aligned} A_\omega &= -k_I^2 (1 + k_{\mu_0} n^2 \pi^2) \{(1 + k_I n^2 \pi^2) [k_C k_{I0}^2 + n^2 \pi^2 (k_C \alpha_6 + k_{I0} \alpha_5)] - k_N \alpha_6 n^2 \pi^2 (1 + k_{\mu_0} n^2 \pi^2)\}, \\ B_\omega &= k_I n^2 \pi^2 (1 + k_{\mu_0} n^2 \pi^2) \{(1 + k_I n^2 \pi^2) [k_C k_{I0} + n^2 \pi^2 (k_{I0} \alpha_2 + k_C \alpha_5)] \\ &\quad - k_N (1 + k_{\mu_0} n^2 \pi^2) [k_C k_{I0} + \alpha_5 n^2 \pi^2]\}, \\ C_\omega &= n^4 \pi^4 (1 + k_{\mu_0} n^2 \pi^2) \{k_N (1 + k_{\mu_0} n^2 \pi^2) (k_C + \alpha_2 n^2 \pi^2) - k_C \alpha_2 n^2 \pi^2 (1 + k_I n^2 \pi^2)\}, \\ \frac{\alpha_3}{\alpha_4} &= \frac{1 + (k_{\mu_0} + k_I) n^2 \pi^2 + k_{\mu_0} k_I n^4 \pi^4}{1 + 2k_{\mu_0} n^2 \pi^2 + k_{\mu_0}^2 n^4 \pi^4}. \end{aligned} \quad (71)$$

By setting $\mu_1 = \mu_0$ we can find the critical temperature ΔT_{cr} from (61) as

$$k_I = \frac{k_N (1 + k_{\mu_0} n^2 \pi^2) (k_C + \alpha_2 n^2 \pi^2) - k_C \alpha_2 n^2 \pi^2}{k_C \alpha_2 n^4 \pi^4}. \quad (72)$$

In this case, when the ratio is $l_\mu = l^2/\mu_0 = l^2/\mu_1 = 1$, the parameters of the system are

$$\begin{aligned} A_\omega &= -k_I^2(1 + k_{\mu 0} n^2 \pi^2)^2 \{k_C k_{I0}^2 + n^2 \pi^2 [k_{I0} \alpha_5 + \alpha_6 (k_C - k_N)]\}, \\ B_\omega &= k_I n^2 \pi^2 (1 + k_{\mu 0} n^2 \pi^2)^2 \{k_C k_{I0} (1 - k_N) + n^2 \pi^2 [k_{I0} \alpha_2 + \alpha_5 (k_C - k_N)]\}, \\ C_\omega &= n^4 \pi^4 (1 + k_{\mu 0} n^2 \pi^2)^2 [k_C k_N - \alpha_2 n^2 \pi^2 (k_C - k_N)], \\ \frac{\alpha_3}{\alpha_4} &= 1, \end{aligned} \quad (73)$$

and the natural frequency does not depend on the nonlocal parameters μ_0 and μ_1 , but also not on the strain gradient length scale l . The natural frequencies of the system are equal to the frequencies for the case of the classical continuum theory.

Case 5 (strain gradient theory). In the case where the nonlocal parameters are zero ($\mu_1 = \mu_0 = 0$) the parameters of the system are

$$\begin{aligned} A_\omega &= -k_I^2 \{ (1 + k_I n^2 \pi^2) [k_C k_{I0}^2 + n^2 \pi^2 (k_C \alpha_6 + k_{I0} \alpha_5)] - k_N \alpha_6 n^2 \pi^2 \}, \\ B_\omega &= k_I n^2 \pi^2 \{ (1 + k_I n^2 \pi^2) [k_C k_{I0} + n^2 \pi^2 (k_{I0} \alpha_2 + k_C \alpha_5)] - k_N [k_C k_{I0} + \alpha_5 n^2 \pi^2] \}, \\ C_\omega &= n^4 \pi^4 \{ k_N (k_C + \alpha_2 n^2 \pi^2) - k_C \alpha_2 n^2 \pi^2 (1 + k_I n^2 \pi^2) \}, \\ \frac{\alpha_3}{\alpha_4} &= 1 + k_I n^2 \pi^2. \end{aligned} \quad (74)$$

By setting $\mu_1 = \mu_0 = 0$ we can find the critical temperature ΔT_{cr} from (61) as

$$k_l = \frac{k_N (k_C + \alpha_2 n^2 \pi^2) - k_C \alpha_2 n^2 \pi^2}{k_C \alpha_2 n^4 \pi^4}. \quad (75)$$

3. Results and discussion

This section examines the influence of temperature change, FG distribution and small-scale effect on the nondimensional natural frequencies. Varying amounts of small-scale parameters are observed and the variations of the critical buckling temperature and nondimensional natural frequencies with respect to the variations of small-scale parameters are discussed. The functionally graded nanobeam is composed of metal (SUS 304) and ceramic (Si_3N_4), where its bottom surface is pure metal and top surface is pure ceramic nitride. The considered beam has the following dimensions: length $L = 10$ nm, width $b = 1$ nm and thickness h varies.

The validity of the proposed method is confirmed by comparing the obtained results with those from the literature [Thai 2012; Rahmani and Pedram 2014]. First, for this purpose, the same parameters are used as in [Thai 2012]. A comparison of the fundamental nondimensional natural frequency for the SS nanobeam is shown in Table 2 for different values of $k_{\mu 0} = 0, 0.01, 0.02, 0.03$ and for ratios $L/h = 5, 10, 20, 100$. The results that are compared are derived from expression (52) for parameter values (62), (65) and $k_N = 0$.

Similarly, a comparison of the results for the FG simply supported nanobeam is given in Table 2 for different values of $k_{\mu 0} = 0, 0.01, 0.02, 0.03$, ratio $L/h = 50$ and the power-law exponent $p = 0, 0.5, 1, 5$. The results that are compared are derived from expression (60) for parameter values (62) and $k_N = 0$. The

k_{μ_0}	L/h				
	5	10	20	100	
0	9.274405 (9.2740)	9.707484 (9.7075)	9.828127 (9.8281)	9.867933 (9.8679)	
0.01	8.848045 (8.8477)	9.261214 (9.2612)	9.376311 (9.3763)	9.414286 (9.4143)	
0.02	8.475550 (8.4752)	8.871325 (8.8713)	8.981576 (8.9816)	9.017953 (9.0179)	
0.03	8.663606 (8.6636)	6.799808 (6.7998)	6.141394 (6.1414)	5.216644 (5.2166)	

Table 2. Comparison with [Thai 2012] of the nondimensional fundamental frequency for a SS FG nanobeam with various nonlocal parameters μ_0 and ratios L/h .

k_{μ_0}	p				
	0	0.5	1	5	
0	9.863157 (9.8631)	7.741301 (7.7413)	6.991723 (6.9917)	5.938935 (5.9389)	
0.01	9.409730 (9.4097)	7.385419 (7.3854)	6.670301 (6.6703)	5.665911 (5.6659)	
0.02	9.013589 (9.0136)	7.074500 (7.0745)	6.389487 (6.3895)	5.427381 (5.4274)	
0.03	8.663606 (8.6636)	6.799808 (6.7998)	6.141394 (6.1414)	5.216644 (5.2166)	

Table 3. Comparison with [Rahmani and Pedram 2014] of the nondimensional fundamental frequency for a SS FG nanobeam with various nonlocal parameters μ_0 and power-law indices p when ratio $L/h = 50$.

same parameters of functionally graded material constituents (steel and alumina) are used as in [Rahmani and Pedram 2014].

Furthermore, in order to validate the results of the present work, equation (63) is solved by considering $l = 0$ and $\mu_1 = 0$, and the results of the critical buckling temperature are compared with the literature [Ebrahimi and Salari 2016] and tabulated in tables 4–6. The influence of the gradient indices p and nonlocal parameter μ_0 on the critical buckling temperature ΔT_{cr} and nondimensional natural frequencies for the simply supported FG nanobeam is considered in detail in [Ebrahimi and Salari 2016]. Here, the effects of different parameters such as the higher-order nonlocal parameter μ_1 and the strain gradient length scale l on the thermal buckling of the FG nanobeam are investigated.

Tables 4–6 present the critical buckling temperature of the simply supported FG nanobeam for various values of the nonlocal parameters and strain gradient scale ($\mu_0 = 0, 1, 2, 3$; $\mu_1 = 0, 1, 2, 3$; $l^2 = 0, 1, 2, 3$) based on the present method, for UTR, LTR and NLTR. It can be concluded from the results in tables 4–6 that an increase in the strain gradient length scale leads to an increase in the critical buckling temperature. Therefore, it can be concluded that an increase in the nonlocal scale parameters μ_0 and the higher-order nonlocal scale parameter μ_1 leads to a decrease in the critical buckling temperature. Variations of the critical buckling temperature ΔT_{cr} of the simply supported FG nanobeam with respect to the nonlocal parameter μ_0 for different values of the power-law index (Eringen's nonlocal continuum theory, $l = 0$, $\mu_1 = 0$) are presented in Figure 2. Examining this figure, it can be concluded that an increase in the nonlocal parameter μ_0 leads to a decrease in the critical buckling temperature. In addition, it can be seen that ΔT_{cr} decreases with the increasing power-law index.

μ_0 (nm ²)	μ_1 (nm ²)	l^2 (nm ²)			
		0	1	2	3
0	0	28.5602 (29.1086)	31.3219	34.0737	36.8153
	1	28.5602	31.0742	33.5801	36.0777
	2	28.5602	30.8673	33.1675	35.4608
	3	28.5602	30.6919	32.8176	34.9375
1	0	26.0379 (26.4938)	28.8087	31.5695	34.3207
	1	26.0379	28.5602	31.0742	33.5802
	2	26.0379	28.3526	30.6603	32.9612
	3	26.0379	28.1766	30.3093	32.4362
2	0	23.9251 (24.3100)	26.7035	29.4718	32.2301
	1	23.9251	26.4543	28.9752	31.4878
	2	23.9251	26.2462	28.5602	30.8672
	3	23.9251	26.0697	28.2082	30.3408
3	0	22.1296 (22.4588)	24.9144	27.6892	30.4538
	1	22.1296	24.6646	27.1914	29.7098
	2	22.1296	24.6228	26.7754	29.0878
	3	22.1296	24.2791	26.4226	28.5602

Table 4. Nonlocality parameters and strain gradient length scale effects on the ΔT_{cr} (K) of the SS FG nanobeam in the UTR case when $p = 1$ and $L/h = 50$.

μ_0 (nm ²)	μ_1 (nm ²)	l^2 (nm ²)			
		0	1	2	3
0	0	49.0533 (50.4274)	54.7761	60.4733	66.1440
	1	49.0533	54.2631	59.4516	64.6183
	2	49.0533	53.8345	58.5977	63.3430
	3	49.0533	53.4710	57.8734	62.2606
1	0	43.8219 (44.9580)	49.5684	55.2889	60.9846
	1	43.8219	49.0533	54.2631	59.4520
	2	43.8219	48.6229	53.4057	58.1707
	3	43.8219	48.2579	52.6784	57.0837
2	0	39.4363 (40.3903)	45.2027	50.9429	56.6569
	1	39.4363	44.6858	49.9135	55.1196
	2	39.4363	44.2539	49.0533	53.8343
	3	39.4363	43.8877	48.3235	52.7436
3	0	35.7065 (36.5182)	41.4901	47.2472	52.9776
	1	35.7065	40.9716	46.2148	51.4360
	2	35.7065	40.5385	45.3520	50.1470
	3	35.7065	40.1712	44.6201	49.0533

Table 5. Nonlocality parameters and strain gradient length scale effects on the ΔT_{cr} (K) of the SS FG nanobeam in the LTR case when $p = 1$ and $L/h = 50$.

μ_0 (nm ²)	μ_1 (nm ²)	l^2 (nm ²)			
		0	1	2	3
0	0	50.8666 (52.0963)	56.8402	62.7871	68.7142
	1	50.8666	56.3045	61.7195	67.1184
	2	50.8666	55.8581	60.8287	65.7855
	3	50.8666	55.4810	60.0705	64.6536
1	0	45.4148 (46.4459)	51.4038	57.3710	63.3165
	1	45.4148	50.8666	56.3006	61.7162
	2	45.4148	50.4179	55.4061	60.3786
	3	45.4148	50.0375	54.6474	59.2440
2	0	40.8519 (41.7270)	46.8540	52.8351	58.7987
	1	40.8519	46.3160	51.7616	57.1936
	2	40.8519	45.8665	50.8666	55.8520
	3	40.8519	45.4853	50.1042	54.7138
3	0	36.9746 (37.7267)	42.9889	49.3428	54.9579
	1	36.9746	42.4489	47.9091	53.3495
	2	36.9746	41.9978	47.0107	52.0053
	3	36.9746	41.6153	46.2487	50.8666

Table 6. Nonlocality parameters and strain gradient length scale effects on the ΔT_{cr} (K) of the SS FG nanobeam in the NLTR case when $p = 1$ and $L/h = 50$.

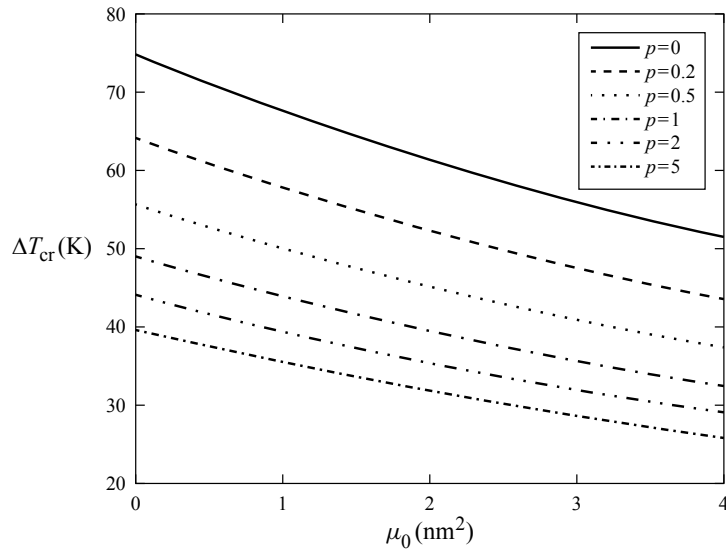


Figure 2. Variation of the critical buckling temperature of the SS FG nanobeam with respect to the nonlocal parameter μ_0 for different values of the power-law index and LNR ($p = 1$, $L/h = 50$, $\mu_1 = 0$, $l^2 = 0$).

It can be further concluded from tables 4–6 that a decrease in the strain gradient scale l and an increase in the higher-order nonlocal scale parameter μ_1 lead to a decrease in the critical buckling temperature. With the increasing strain gradient scale l , the effect of increasing the higher-order nonlocal parameter μ_1 is compared with the effect of increasing the nonlocal parameter μ_0 . It can still be concluded that at small values of the strain gradient scale l , increasing the nonlocal parameter μ_0 has more effects on decreasing the critical buckling temperature than increasing the higher-order nonlocal parameter μ_1 . In cases where the strain gradient length scale is zero (see (70)), variations on the higher-order nonlocal parameter μ_1 will have no effect on the critical buckling temperature. To have a better understanding of this issue, variations of the critical buckling temperature of the FG nanobeam are plotted in Figure 3 with respect to increasing the strain length scale and different values of the nonlocal parameters μ_0 and μ_1 . For the same reason, Figure 4 presents variations of the critical buckling temperature ΔT_{cr} with respect to the new scale factor

$$l_\mu = \frac{l^2}{\mu}, \tag{76}$$

for different values of the nonlocal parameter where $\mu = \mu_0 = \mu_1$. It can be concluded that the critical buckling temperature is smaller than the result of the classical solution when the nonlocal parameter is smaller than the strain length scale ($l_\mu < 1$); the critical buckling temperature is larger than the result of the classical solution when the nonlocal parameter is larger than the strain gradient length scale ($l_\mu > 1$). When the nonlocal parameter is equal to the strain gradient length scale $l_\mu = 1$, the critical buckling temperature is equal to that of the classical solution. Also, when $l_\mu = 0$, the results are equal to those from the nonlocal elasticity theory.

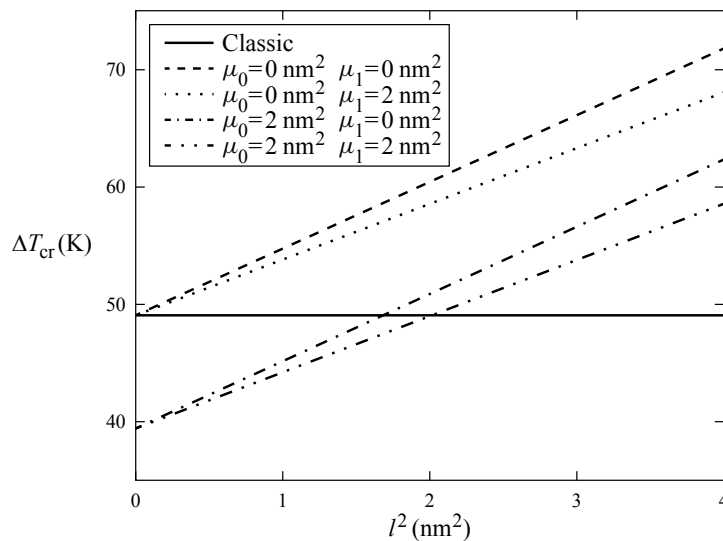


Figure 3. Variation of the critical buckling temperature of the SS FG nanobeam with respect to the strain length scale for different values of the nonlocal parameters and LNR ($p = 1$ $L/h = 50$).

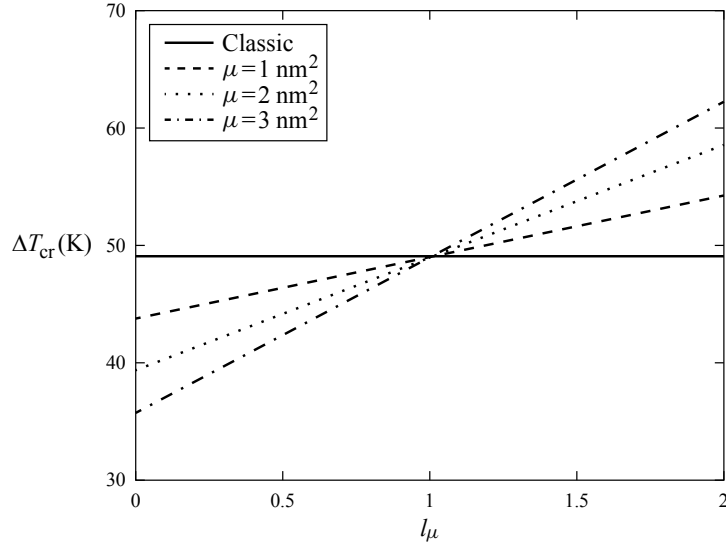


Figure 4. Variation of the critical buckling temperature of the SS FG nanobeam with respect to ratio l_μ , strain length scale for different values of the nonlocal parameters and LNR ($p = 1$ $L/h = 50$ $\mu_0 = \mu_1 = \mu$).

In order to investigate the vibration characteristics of the simply supported FG nanobeam, the first three nondimensional frequencies are presented in tables 7–15. Tables 7–9 present the natural frequencies of the simply supported FG nanobeam subjected to a uniform temperature rise for various values of the nonlocal parameters and the strain gradient length scale parameter ($\mu_0 = 0, 1, 2, 3$; $\mu_1 = 0, 1, 2, 3$; $l^2 = 0, 1, 2, 3$) based on the present method. Also, tables 10–12 and tables 13–15 present the natural frequencies of the simply supported FG nanobeam subjected to a linear and a nonlinear temperature rise, respectively. It can be concluded from the results given in these tables that an increase in the strain gradient length scale l leads to an increase in the nondimensional frequency. On the other hand, an increase in the nonlocal scale parameters μ_0 and the higher-order nonlocal scale parameter μ_1 leads to a decrease in the nondimensional natural frequency. It can still be concluded that at small values of the strain gradient scale l , increasing the nonlocal parameter μ_0 has more effects on decreasing the nondimensional frequency than increasing the higher-order nonlocal parameter μ_1 . With the increasing strain gradient scale l , increasing the nonlocal parameter μ_1 has more effects on decreasing the nondimensional frequency than increasing the higher-order nonlocal parameter μ_0 . To have a better understanding of this issue, variations of the frequency ratio

$$k_{\omega n} = \frac{\omega_n}{\omega_{nc}}, \quad (77)$$

are plotted in figures 5–7 with respect to the nonlocal scale parameters μ_0 for different values of the strain length scale l and the nonlocal parameter μ_1 , where ω_n is the nondimensional frequency calculated using the nonlocal theory (for the parameters of system (59)) and ω_{nc} is the nondimensional frequency calculated using the classical local theory (for the parameters of system (64)). This frequency ratio serves as an index to quantitatively estimate the effects of the nonlocal parameters μ_0 and μ_1 , and the

μ_0 (nm ²)	μ_1 (nm ²)	l^2 (nm ²)			
		0	1	2	3
0	0	5.4110 (5.4110)	5.7233	6.0195	6.3018
	1	5.4110	5.6960	5.9674	6.2270
	2	5.4110	5.6730	5.9235	6.1638
	3	5.4110	5.6535	5.8860	6.1097
1	0	5.1101 (5.1102)	5.4398	5.7506	6.0454
	1	5.1101	5.4110	5.6960	5.9674
	2	5.1101	5.3868	5.6500	5.9014
	3	5.1101	5.3663	5.6107	5.8449
2	0	4.8446 (4.8446)	5.1911	5.5159	5.8226
	1	4.8446	5.1609	5.4500	5.7416
	2	4.8446	5.1356	5.4110	5.6730
	3	4.8446	5.1140	5.3700	5.6142
3	0	4.6075 (4.6075)	4.9706	5.3089	5.6269
	1	4.6075	4.9391	5.2497	5.5430
	2	4.6075	4.9126	5.1998	5.4720
	3	4.6075	4.8900	5.1571	5.4110

Table 7. Nonlocality parameters and strain gradient length scale effects on the first nondimensional frequency ω_1 in the UTR case when $p = 1$, $L/h = 20$, $\Delta T = 30$ K.

strain length scale l on the vibration solution. It can be clearly seen from the figures that the frequency ratio is less than unity when $l = 0$, regardless of the values of the nonlocal parameters μ_0 and μ_1 . The frequency ratio has higher values for higher frequencies. It is observed that increasing the nonlocal parameters will decrease the frequency ratio and decreasing the strain gradient length scale will decrease the frequency ratio. With an increase in the order of frequency, the greatest influence on the frequency ratio is exerted by the nonlocal parameter μ_1 . In the cases where the strain gradient length scale is zero (see (70)), variations of the nonlocal parameter μ_1 will have no effect on the frequency ratio. In the case when $l^2 = \mu_0 = \mu_1$, the frequency ratio is one for all orders of frequency and all values of the nonlocal parameters μ_0 and μ_1 and the strain length scale l .

4. Conclusions

This paper investigates the thermal buckling and vibration of the FG nanobeam subjected to different temperature distributions in the through-thickness direction (UTR, LNR and NLTR). By using the variational approach, the equations of motion are obtained based on the Timoshenko beam theory within the framework of the higher-order nonlocal strain gradient theory. The effect of the nonlocal parameters and strain gradient length scale on the critical buckling temperature and nondimensional frequency is observed. Numerical results are presented for certain characteristics of the rectangular cross-section of the beam. It is concluded that an increase in the nonlocal parameters will decrease the critical buckling temperature and nondimensional frequency, while a decrease in the strain gradient length scale will lead to a decrease in the critical buckling temperature and nondimensional natural frequency. For small values

μ_0 (nm ²)	μ_1 (nm ²)	l^2 (nm ²)			
		0	1	2	3
0	0	22.9433 (22.9447)	27.2682	30.9954	34.3203
	1	22.9433	26.1168	28.9445	31.5195
	2	22.9433	25.4508	27.7325	29.8402
	3	22.9433	25.0162	26.9301	28.7166
1	0	19.2535 (19.2547)	24.2458	28.3729	31.9716
	1	19.2535	22.9433	26.1168	28.9445
	2	19.2535	22.1821	24.7668	27.1062
	3	19.2535	21.6821	23.8649	25.8641
2	0	16.8433 (16.8443)	22.3799	26.7959	30.5807
	1	16.8433	20.9617	24.3944	27.4004
	2	16.8433	20.1257	22.9433	25.4508
	3	16.8433	19.5733	21.9666	24.1236
3	0	15.1044 (15.1054)	21.1022	25.7384	29.6585
	1	15.1044	19.5918	23.2279	26.3672
	2	15.1044	18.6947	21.6988	24.3349
	3	15.1044	18.0986	20.6634	22.9433

Table 8. Nonlocality parameters and strain gradient length scale effects on the second nondimensional frequency ω_2 in the UTR case when $p = 1$, $L/h = 20$, $\Delta T = 30$ K.

μ_0 (nm ²)	μ_1 (nm ²)	l^2 (nm ²)			
		0	1	2	3
0	0	51.2311 (51.2374)	70.7310	85.9135	98.7896
	1	51.2311	62.3227	71.7190	80.0194
	2	51.2311	59.0016	65.8615	72.0715
	3	51.2311	57.2152	62.6300	67.6126
1	0	36.9478 (36.9524)	61.1833	78.2409	92.1949
	1	36.9478	51.2311	62.3227	71.7190
	2	36.9478	47.1349	55.4820	62.7280
	3	36.9478	44.8786	51.6046	57.5498
2	0	30.1914 (30.1952)	57.3565	75.2863	89.7010
	1	30.1914	46.5941	58.5705	68.4835
	2	30.1914	42.0485	51.2311	59.0016
	3	30.1914	39.5027	47.0044	53.4636
3	0	26.0345 (26.0379)	55.2815	73.7177	88.3886
	1	26.0345	44.0146	56.5400	66.7553
	2	26.0345	39.1708	48.8969	56.9865
	3	26.0345	36.4244	44.4487	51.2311

Table 9. Nonlocality parameters and strain gradient length scale effects on the third nondimensional frequency ω_3 in the UTR case when $p = 1$, $L/h = 20$, $\Delta T = 30$ K.

μ_0 (nm ²)	μ_1 (nm ²)	l^2 (nm ²)			
		0	1	2	3
0	0	5.6111 (5.6105)	5.9136	6.2013	6.4763
	1	5.6111	5.8871	6.1506	6.4033
	2	5.6111	5.8648	6.1080	6.3418
	3	5.6111	5.8459	6.0716	6.2891
1	0	5.3209 (5.3204)	5.6390	5.9400	6.2265
	1	5.3209	5.6111	5.8871	6.1506
	2	5.3209	5.5878	5.8425	6.0865
	3	5.3209	5.5679	5.8044	6.0316
2	0	5.0659 (5.0654)	5.3989	5.7126	6.0100
	1	5.0659	5.3699	5.6576	5.9313
	2	5.0659	5.3455	5.6111	5.8648
	3	5.0659	5.3247	5.5715	5.8078
3	0	4.8391 (4.8388)	5.1868	5.5126	5.8201
	1	4.8391	5.1565	5.4555	5.7389
	2	4.8391	5.1311	5.4073	5.6701
	3	4.8391	5.1094	5.3662	5.6111

Table 10. Nonlocality parameters and strain gradient length scale effects on the first nondimensional frequency ω_1 in the LTR case when $p = 1$, $L/h = 20$, $\Delta T = 30$ K.

μ_0 (nm ²)	μ_1 (nm ²)	l^2 (nm ²)			
		0	1	2	3
0	0	23.1537 (23.1492)	27.4544	31.1673	34.4827
	1	23.1537	26.3086	29.1237	31.6897
	2	23.1537	25.6460	27.9167	30.016
	3	23.1537	25.2138	27.1178	28.8967
1	0	19.4947 (19.4913)	24.4479	28.5544	32.1404
	1	19.4947	23.1537	26.3086	29.1237
	2	19.4947	22.3979	24.9658	27.2931
	3	19.4947	21.9017	24.0692	26.0571
2	0	17.1127 (17.1100)	22.5942	26.9843	30.7540
	1	17.1127	21.1871	24.5956	27.5860
	2	17.1127	20.3585	23.1537	25.6460
	3	17.1127	19.8113	22.1840	24.3264
3	0	15.4002 (15.3980)	21.3265	25.9321	29.8350
	1	15.4002	19.8296	23.4363	26.5577
	2	15.4002	18.9417	21.9183	24.5364
	3	15.4002	18.3523	20.8914	23.1537

Table 11. Nonlocality parameters and strain gradient length scale effects on the second nondimensional frequency ω_2 in the LTR case when $p = 1$, $L/h = 20$, $\Delta T = 30$ K.

μ_0 (nm ²)	μ_1 (nm ²)	l^2 (nm ²)			
		0	1	2	3
0	0	51.4739 (51.4699)	70.9453	86.1214	98.9978
	1	51.4739	62.5454	71.9325	80.2287
	2	51.4739	59.229	66.0801	72.2847
	3	51.4739	57.4455	62.8523	67.8294
1	0	37.2452 (37.2400)	61.4074	78.4509	92.4024
	1	37.2452	51.4739	62.5454	71.9325
	2	37.2452	47.3889	55.7155	62.9502
	3	37.2452	45.1401	51.8464	57.7795
2	0	30.5377 (30.5340)	57.5866	75.4976	89.9086
	1	30.5377	46.8499	58.7985	68.6995
	2	30.5377	42.3209	51.4739	59.229
	3	30.5377	39.7866	47.2589	53.7012
3	0	26.4253 (26.4225)	55.5154	73.9299	88.5962
	1	26.4253	44.2793	56.7716	66.9729
	2	26.4253	39.4563	49.1458	57.2172
	3	26.4253	36.7249	44.7118	51.4739

Table 12. Nonlocality parameters and strain gradient length scale effects on the third nondimensional frequency ω_3 in the LTR case when $p = 1$, $L/h = 20$, $\Delta T = 30$ K.

μ_0 (nm ²)	μ_1 (nm ²)	l^2 (nm ²)			
		0	1	2	3
0	0	5.6220 (5.6135)	5.9239	6.2112	6.4857
	1	5.6220	5.8974	6.1605	6.4129
	2	5.6220	5.8752	6.118	6.3514
	3	5.6220	5.8563	6.0816	6.2988
1	0	5.3324 (5.3246)	5.6498	5.9503	6.2363
	1	5.3324	5.6220	5.8974	6.1605
	2	5.3324	5.5987	5.8529	6.0965
	3	5.3324	5.5789	5.8149	6.0418
2	0	5.0778 (5.0707)	5.4102	5.7233	6.0201
	1	5.0778	5.3812	5.6683	5.9416
	2	5.0778	5.3568	5.6220	5.8752
	3	5.0778	5.3361	5.5824	5.8183
3	0	4.8516 (4.8450)	5.1985	5.5236	5.8306
	1	4.8516	5.1683	5.4666	5.7495
	2	4.8516	5.1429	5.4186	5.6808
	3	4.8516	5.1213	5.3775	5.6220

Table 13. Nonlocality parameters and strain gradient length scale effects on the first nondimensional frequency ω_1 in the NLTR case when $p = 1$, $L/h = 20$, $\Delta T = 30$ K.

μ_0 (nm ²)	μ_1 (nm ²)	l^2 (nm ²)			
		0	1	2	3
0	0	23.1647 (23.1233)	27.4639	31.1759	34.4906
	1	23.1647	26.3184	29.1327	31.6982
	2	23.1647	25.6560	27.9260	30.0249
	3	23.1647	25.2240	27.1274	28.9058
1	0	19.5075 (19.4735)	24.4583	28.5636	32.1488
	1	19.5075	23.1647	26.3184	29.1327
	2	19.5075	22.4092	24.9761	27.3027
	3	19.5075	21.9133	24.0799	26.0670
2	0	17.1272 (17.0980)	22.6054	26.9939	30.7626
	1	17.1272	21.1990	24.6060	27.5955
	2	17.1272	20.3708	23.1647	25.6560
	3	17.1272	19.8239	22.1954	24.3369
3	0	15.4161 (15.3906)	21.3383	25.9420	29.8439
	1	15.4161	19.8422	23.4472	26.5674
	2	15.4161	18.9549	21.9299	24.5469
	3	15.4161	18.3659	20.9034	23.1647

Table 14. Nonlocality parameters and strain gradient length scale effects on the second nondimensional frequency ω_2 in the NLTR case when $p = 1$, $L/h = 20$, $\Delta T = 30$ K.

μ_0 (nm ²)	μ_1 (nm ²)	l^2 (nm ²)			
		0	1	2	3
0	0	51.4858 (51.3939)	70.9549	86.1302	99.0061
	1	51.4858	62.5557	71.942	80.2377
	2	51.4858	59.2397	66.0901	72.2942
	3	51.4858	57.4565	62.8626	67.8393
1	0	37.2606 (37.1957)	61.4179	78.4600	92.4109
	1	37.2606	51.4858	62.5557	71.9420
	2	37.2606	47.4016	55.7267	62.9605
	3	37.2606	45.1532	51.8582	57.7905
2	0	30.5561 (30.5042)	57.5976	75.5069	89.9172
	1	30.5561	46.8626	58.8094	68.7093
	2	30.5561	42.3347	51.4858	59.2397
	3	30.5561	39.8012	47.2715	53.7127
3	0	26.4462 (26.4025)	55.5267	73.9393	88.6049
	1	26.4462	44.2926	56.7826	66.9828
	2	26.4462	39.4710	49.1581	57.2282
	3	26.4462	36.7405	44.725	51.4858

Table 15. Nonlocality parameters and strain gradient length scale effects on the third nondimensional frequency ω_3 in the NLTR case when $p = 1$, $L/h = 20$, $\Delta T = 30$ K.

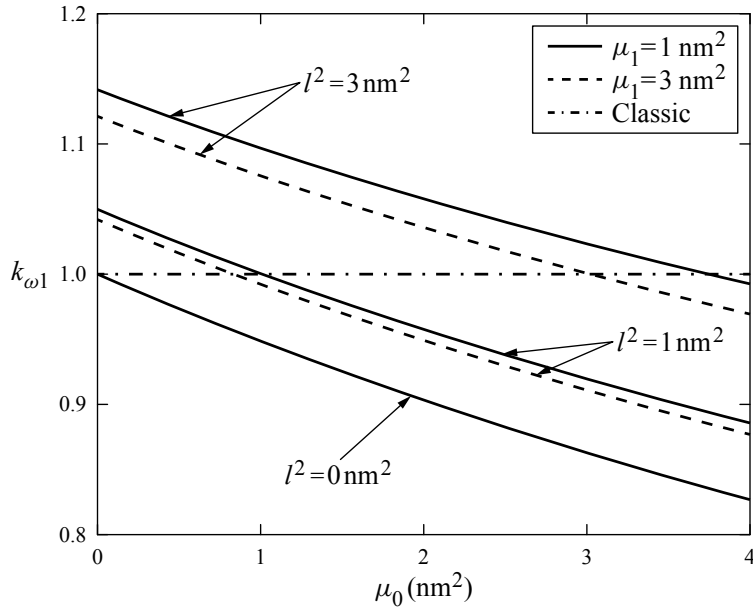


Figure 5. Variation of the frequency ratio for the first nondimensional frequency of the SS FG nanobeam with respect to the nonlocal parameter μ_0 for different values of μ_1 and l^2 and LNR ($p = 1$, $L/h = 50$).

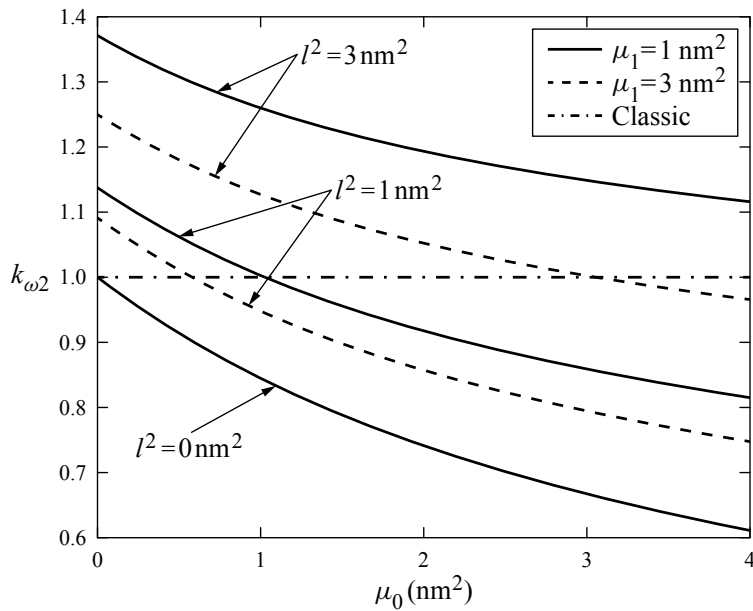


Figure 6. Variation of the frequency ratio for the second nondimensional frequency of the SS FG nanobeam with respect to the nonlocal parameter μ_0 for different values of μ_1 and l^2 and LNR ($p = 1$, $L/h = 50$).

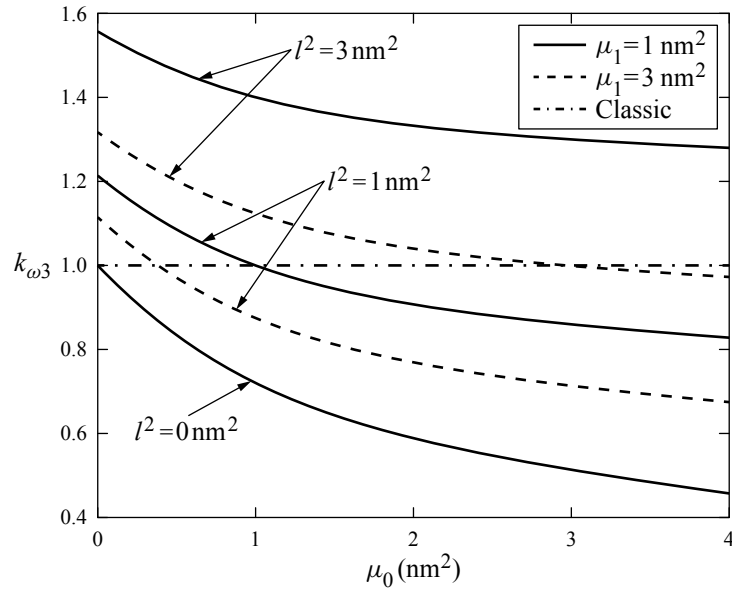


Figure 7. Variation of the frequency ratio for the third nondimensional frequency of the SS FG nanobeam with respect to the nonlocal parameter μ_0 for different values of μ_1 and l^2 and LNR ($p = 1$, $L/h = 50$).

of the strain gradient scale, the dominant influence is exerted by the nonlocal parameter, while for higher values, the dominant influence is shown by the higher-order nonlocal parameter. If nonlocal parameters are equal, then for the values of the strain gradient scale that are smaller than the nonlocal parameter, the critical buckling temperature and nondimensional frequency are lower than in the classical solution, and for the values of the strain gradient scale that are higher than the nonlocal parameter, the critical buckling temperature and nondimensional frequency are higher than in the classical solution. In the case when the strain gradient length scale is zero, the higher-order nonlocal parameters practically have no effect on the critical buckling temperature and nondimensional frequency.

Acknowledgement

This research was supported by the research grant of the Serbian Ministry of Science and Environmental Protection under the number OI 174011.

References

- [Aifantis 1992] E. C. Aifantis, "On the role of gradients in the localization of deformation and fracture", *Int. J. Eng. Sci.* **30**:10 (1992), 1279–1299.
- [Al-shujairi and Mollamahmutoğlu 2018] M. Al-shujairi and Ç. Mollamahmutoğlu, "Buckling and free vibration analysis of functionally graded sandwich micro-beams resting on elastic foundation by using nonlocal strain gradient theory in conjunction with higher order shear theories under thermal effect", *Compos. B Eng.* **154** (2018), 292–312.
- [Alshehri and Hill 2017] M. H. Alshehri and J. M. Hill, "Suction energy for double-stranded DNA inside single-walled carbon nanotubes", *Quart. J. Mech. Appl. Math.* **70**:4 (2017), 387–400.

- [Chen et al. 2019] W. Chen, L. Wang, and H.-L. Dai, “Nonlinear free vibration of nanobeams based on nonlocal strain gradient theory with the consideration of thickness-dependent size effect”, *J. Mech. Mater. Struct.* **14**:1 (2019), 119–137.
- [Ebrahimi and Haghi 2017] F. Ebrahimi and P. Haghi, “Wave propagation analysis of rotating thermoelastically-actuated nanobeams based on nonlocal strain gradient theory”, *Acta Mech. Solida Sin.* **30**:6 (2017), 647–657.
- [Ebrahimi and Salari 2015a] F. Ebrahimi and E. Salari, “Thermal buckling and free vibration analysis of size dependent Timoshenko FG nanobeams in thermal environments”, *Compos. Struct.* **128** (2015), 363–380.
- [Ebrahimi and Salari 2015b] F. Ebrahimi and E. Salari, “Nonlocal thermo-mechanical vibration analysis of functionally graded nanobeams in thermal environment”, *Acta Astronaut.* **113** (2015), 29–50.
- [Ebrahimi and Salari 2016] F. Ebrahimi and E. Salari, “Effect of various thermal loadings on buckling and vibrational characteristics of nonlocal temperature-dependent functionally graded nanobeams”, *Mech. Adv. Mater. Struct.* **23**:12 (2016), 1379–1397.
- [Eringen 1983] A. C. Eringen, “On differential equations of nonlocal elasticity and solutions of screw dislocation and surface waves”, *J. Appl. Phys.* **54**:9 (1983), 4703–4710.
- [Eringen 2002] A. C. Eringen, *Nonlocal continuum field theories*, Springer, New York, NY, 2002.
- [Fu et al. 2012] Y. Fu, J. Wang, and Y. Mao, “Nonlinear analysis of buckling, free vibration and dynamic stability for the piezoelectric functionally graded beams in thermal environment”, *Appl. Math. Model.* **36**:9 (2012), 4324–4340.
- [Ghazavi et al. 2018] M. R. Ghazavi, H. Molki, and A. Ali Beigloo, “Nonlinear analysis of the micro/nanotube conveying fluid based on second strain gradient theory”, *Appl. Math. Model.* **60** (2018), 77–93.
- [Li et al. 2016] L. Li, X. Li, and Y. Hu, “Free vibration analysis of nonlocal strain gradient beams made of functionally graded material”, *Int. J. Eng. Sci.* **102** (2016), 77–92.
- [Li et al. 2018] L. Li, H. Tang, and Y. Hu, “The effect of thickness on the mechanics of nanobeams”, *Int. J. Eng. Sci.* **123** (2018), 81–91.
- [Lim et al. 2015] C. W. Lim, G. Zhang, and J. N. Reddy, “A higher-order nonlocal elasticity and strain gradient theory and its applications in wave propagation”, *J. Mech. Phys. Solids* **78** (2015), 298–313.
- [Lu et al. 2017] L. Lu, X. Guo, and J. Zhao, “Size-dependent vibration analysis of nanobeams based on the nonlocal strain gradient theory”, *Int. J. Eng. Sci.* **116** (2017), 12–24.
- [Mindlin 1964] R. D. Mindlin, “Micro-structure in linear elasticity”, *Arch. Ration. Mech. Anal.* **16**:1 (1964), 51–78.
- [Neek-Amal and Peeters 2010] M. Neek-Amal and F. M. Peeters, “Graphene nanoribbons subjected to axial stress”, *Phys. Rev. B* **82**:8 (2010), 085432.
- [Pavlović et al. 2019a] I. R. Pavlović, R. Pavlović, and G. Janevski, “Dynamic stability and instability of nanobeams based on the higher-order nonlocal strain gradient theory”, *Quart. J. Mech. Appl. Math.* **72**:2 (2019), 157–178.
- [Pavlović et al. 2019b] I. R. Pavlović, R. Pavlović, and G. Janevski, “Mathematical modeling and stochastic stability analysis of viscoelastic nanobeams using higher-order nonlocal strain gradient theory”, *Arch. Mech.* **71**:2 (2019), 137–153.
- [Rahmani and Pedram 2014] O. Rahmani and O. Pedram, “Analysis and modeling the size effect on vibration of functionally graded nanobeams based on nonlocal Timoshenko beam theory”, *Int. J. Eng. Sci.* **77** (2014), 55–70.
- [Şimşek and Yurtcu 2013] M. Şimşek and H. H. Yurtcu, “Analytical solutions for bending and buckling of functionally graded nanobeams based on the nonlocal Timoshenko beam theory”, *Compos. Struct.* **97** (2013), 378–386.
- [Tang et al. 2019] H. Tang, L. Li, Y. Hu, W. Meng, and K. Duan, “Vibration of nonlocal strain gradient beams incorporating Poisson’s ratio and thickness effects”, *Thin-Walled Struct.* **137** (2019), 377–391.
- [Thai 2012] H.-T. Thai, “A nonlocal beam theory for bending, buckling, and vibration of nanobeams”, *Int. J. Eng. Sci.* **52** (2012), 56–64.
- [Touloukian 1967] Y. S. Touloukian (editor), *Thermophysical properties of high temperature solid materials*, vol. 1: Elements, Macmillan, New York, 1967.
- [Trinh et al. 2016] L.-C. Trinh, T. P. Vo, H.-T. Thai, and T.-K. Nguyen, “An analytical method for the vibration and buckling of functionally graded beams under mechanical and thermal loads”, *Compos. B Eng.* **100** (2016), 152–163.
- [Xu et al. 2017] X.-J. Xu, X.-C. Wang, M.-L. Zheng, and Z. Ma, “Bending and buckling of nonlocal strain gradient elastic beams”, *Compos. Struct.* **160** (2017), 366–377.

[Yang et al. 2018] Y. Yang, J. Wang, and Y. Yu, "Wave propagation in fluid-filled single-walled carbon nanotubes on the nonlocal strain gradient theory", *Acta Mech. Solida Sin.* **31**:4 (2018), 484–492.

Received 17 Jul 2019. Revised 5 Dec 2019. Accepted 14 Dec 2019.

GORAN JANEVSKI: gocky.jane@gmail.com

Department of Mechanical Engineering, University of Niš, Univerzitetski trg 2, 18000 Niš, Serbia

IVAN PAVLOVIĆ: ivanp79@gmail.com

Department of Mechanical Engineering, University of Niš, 18000 Niš, Serbia

NIKOLA DESPENIĆ: ndespa91@gmail.com

Department of Mechanical Engineering, University of Niš, 18000 Niš, Serbia

JOURNAL OF MECHANICS OF MATERIALS AND STRUCTURES

msp.org/jomms

Founded by Charles R. Steele and Marie-Louise Steele

EDITORIAL BOARD

ADAIR R. AGUIAR	University of São Paulo at São Carlos, Brazil
KATIA BERTOLDI	Harvard University, USA
DAVIDE BIGONI	University of Trento, Italy
MAENGHYO CHO	Seoul National University, Korea
HUILING DUAN	Beijing University
YIBIN FU	Keele University, UK
IWONA JASIUKEWICZ	University of Illinois at Urbana-Champaign, USA
DENNIS KOCHMANN	ETH Zurich
MITSUTOSHI KURODA	Yamagata University, Japan
CHEE W. LIM	City University of Hong Kong
ZISHUN LIU	Xi'an Jiaotong University, China
THOMAS J. PENCE	Michigan State University, USA
GIANNI ROYER-CARFAGNI	Università degli studi di Parma, Italy
DAVID STEIGMANN	University of California at Berkeley, USA
PAUL STEINMANN	Friedrich-Alexander-Universität Erlangen-Nürnberg, Germany
KENJIRO TERADA	Tohoku University, Japan

ADVISORY BOARD

J. P. CARTER	University of Sydney, Australia
D. H. HODGES	Georgia Institute of Technology, USA
J. HUTCHINSON	Harvard University, USA
D. PAMPLONA	Universidade Católica do Rio de Janeiro, Brazil
M. B. RUBIN	Technion, Haifa, Israel

PRODUCTION production@msp.org

SILVIO LEVY Scientific Editor

Cover photo: Ev Shafir

See msp.org/jomms for submission guidelines.

JoMMS (ISSN 1559-3959) at Mathematical Sciences Publishers, 798 Evans Hall #6840, c/o University of California, Berkeley, CA 94720-3840, is published in 10 issues a year. The subscription price for 2020 is US \$660/year for the electronic version, and \$830/year (+\$60, if shipping outside the US) for print and electronic. Subscriptions, requests for back issues, and changes of address should be sent to MSP.

JoMMS peer-review and production is managed by EditFLOW® from Mathematical Sciences Publishers.

PUBLISHED BY

 **mathematical sciences publishers**
nonprofit scientific publishing

<http://msp.org/>

© 2020 Mathematical Sciences Publishers

Journal of Mechanics of Materials and Structures

Volume 15, No. 1

January 2020

Stress-minimizing holes with a given surface roughness in a remotely loaded elastic plane	SHMUEL VIGDERGAUZ and ISAAC ELISHAKOFF	1
Analytical modeling and computational analysis on topological properties of 1-D phononic crystals in elastic media	MUHAMMAD and C. W. LIM	15
Dynamics and stability analysis of an axially moving beam in axial flow	YAN HAO, HULIANG DAI, NI QIAO, KUN ZHOU and LIN WANG	37
An approximate formula of first peak frequency of ellipticity of Rayleigh surface waves in an orthotropic layered half-space model	TRUONG THI THUY DUNG, TRAN THANH TUAN, PHAM CHI VINH and GIANG KIEN TRUNG	61
Effect of number of crowns on the crush resistance in open-cell stent design	GIDEON PRAVEEN KUMAR, KEPING ZUO, LI BUAY KOH, CHI WEI ONG, YUCHENG ZHONG, HWA LIANG LEO, PEI HO and FANGSEN CUI	75
A dielectric breakdown model for an interface crack in a piezoelectric bimaterial	YURI LAPUSTA, ALLA SHEVELEVA, FRÉDÉRIC CHAPELLE and VOLODYMYR LOBODA	87
Thermal buckling and free vibration of Timoshenko FG nanobeams based on the higher-order nonlocal strain gradient theory	GORAN JANEVSKI, IVAN PAVLOVIĆ and NIKOLA DESPENIĆ	107
A new analytical approach for solving equations of elasto-hydrodynamics in quasicrystals	VALERY YAKHNO	135
Expansion-contraction behavior of a pressurized porohyperelastic spherical shell due to fluid redistribution in the structure wall	VAHID ZAMANI and THOMAS J. PENCE	159



1559-3959(2020)15:1;1-L